Fermi National Accelerator Laboratory

FERMILAB-Pub-94/254-A
August 1994

A Merger Model and Globular Cluster Formation

Sangjin Lee[1], David N. Schramm[1,2], & Grant J. Mathews[3]

[1] *Department of Physics, The University of Chicago*
Chicago, IL 60637

[2] *NASA/Fermilab Astrophysics Center,*
Fermi National Accelerator Laboratory
Batavia, IL 60510

[3] *University of California, Lawrence Livermore National Laboratory*
Livermore, CA 94550

Abstract

We propose a self-consistent model for globular cluster formation in, but not limited to, our Galaxy, based on the merger model of Mathews & Schramm (1993). Stars and star clusters form in bursts at the merging interfaces as protogalactic clouds collide. We describe the formation of those star clusters with a simple schematic ansatz which takes into account the thermal and Kelvin-Helmholtz instabilities. It is shown that this model is consistent with many observational properties such as the age and metallicity distributions of globular clusters, the overall number of globular clusters, and the near constancy of the number of globular clusters in different size host galaxies. Most of the features of this merger model are insensitive to choices of parameters. However, the model does not exhibit two distinct populations of globular clusters, i.e. halo clusters and disk clusters. Possible explanations for this are presented.

Subject headings: cosmology: theory - galaxies: star clusters - Galaxy: formation - Galaxy: globular clusters: general - stars: formation

· Submitted to *The Astrophysical Journal*

1 Introduction

Globular clusters have the focus of considerable study both in cosmology and in astrophysics. Since they are inferred to be among the oldest objects in our Galaxy, their age serves as a lower bound on the age of the Galaxy and the Universe (Chaboyer et al. 1992a; Chaboyer, Sarajedini, & Demarque 1992b; Sandage 1993). The dating of globular clusters has yielded interesting bounds on cosmological parameters, such as the interrelationship between present fraction of the closure density of the Universe Ω_0, and the Hubble constant H_0. Since at least some of globular clusters are extremely old, they also provide information about the early galactic environment and galaxy formation process.

There have been several different models for the origin of globular clusters. Peebles & Dicke (1968) first pointed out that globular clusters might have formed even before the collapse of the protogalaxy, noting the fact that the baryonic Jeans mass right after decoupling is about the size of a globular cluster. However, it cannot explain why there are so few intergalactic globular clusters, if any, and why the properties of globular clusters are correlated with host galaxies. Fall & Rees (1985) suggested that globular clusters may have formed out of thermal instabilities during the collapse of the protogalaxy. In their model, cold dense clouds condense out of hot and tenuous background to form as progenitors of globular clusters. While many theories on globular cluster formation assume a smooth and rapid collapse of the protogalaxy (see e.g. Eggen, Lynden-Bell, & Sandage 1962), there are indications (Searle & Zinn 1978) that the early Galactic environment might have been much more chaotic and violent.

Murray & Lin (1992) have argued that self-gravitating clouds are unstable to fragmentations and spontaneous star formation so that globular clusters must form from sub-Jeans-mass clouds. In subsequent work Murray et al. (1993) have shown that only clouds in a limited mass range ($10^4 M_\odot \lesssim M \lesssim 10^6 M_\odot$) can survive both the Kelvin-Helmholtz (KH) instability (which disrupts the clouds as they move through the hot background medium) and the thermal instability (i.e. spontaneous cooling and star formation) which does not lead to bound clusters. Clouds within the critical mass range will form globular clusters if they are induced into cooling and collapse by collisions of sufficient velocity. In what follows we develop a simple schematic model of protogalactic mergers, to describe globular cluster formation and metallicity within this context.

Mathews & Schramm (1993, called MS hereafter) proposed a schematic merger model for the formation of the halo and chemical evolution of the Galaxy in which the protogalaxy forms by mergers of small subgalactic gas clouds. The mergers during the collapse of the protogalaxy can produce a substantial number of stars in addition to the normal star formation activity within the gas clouds. Using this merger model, they could provide insight into a number of problems, such as the apparent discrepancy of the various age estimators of the Galaxy, the G-dwarf problem, etc.

The formation and evolution of globular clusters arises quite naturally in the framework of such a merger model. Here we explore the consequences of this merger model on the formation of globular clusters.

2 Formalism

An exact analytic treatment of the merging processes is impossible. A detailed physical description requires numerical hydrodynamic simulations using widely varying initial conditions, etc. (e.g. Lin & Murray 1992; Brown, Burkert, & Truran 1991) The next best, however, is suppose a reasonable schematic model which encompasses the basic features of the large scale numerical simulations.

Following the simple kinematical argument given in MS, the merger rate per protogalactic cloud can be approximated

$$\lambda_m = \frac{1}{2}\frac{N-1}{V}\sigma v\left(1 - e^{-\frac{t-t_0}{t_{vir}}}\right) \tag{1}$$

where N is the number of clouds, V is the volume of the protogalaxy, σ is the merger cross section, which is approximated by a geometric cross section, and v is the virial velocity which is related to the median radius of the protogalaxy by

$$v^2 \simeq 0.4\frac{GM}{R_h}. \tag{2}$$

The exponential factor in eq. [1] allows for the fact that the protogalactic clouds do not form and virialize instantaneously, but require a collapse time, $t_{vir} \sim 10^8$ yr. We also assume that the mass of the protogalaxy is $\sim 4 \times 10^{11} M_\odot$, and the initial mass of an average protogalactic fragment cloud is $10^6 M_\odot$, following MS. If the bulk of the mass of our Galaxy is in the form of non-baryonic dark matter, one must allow for the fact that only a fraction of the $4 \times 10^{11} M_\odot$ total mass is baryonic, but the essence of the model remains. We will concentrate here on the case of a purely baryonic halo, and also consider the possibility of non-baryonic dark matter later in section 3.1.

The total stellar birthrate function is written as

$$\psi(t) = \alpha\psi_m + \beta\psi_c \tag{3}$$

where ψ_m represents the star birthrate induced by mergers, and is given as

$$\psi_m \propto \lambda_m, \tag{4}$$

and ψ_c represents the quiescent star formation rate due to self-regulated star formation and/or fragmentations of larger clouds, which is taken to be

$$\psi_c \sim \rho_g^{1/2}. \tag{5}$$

The age of the Galaxy is taken to be $\sim$ 15 Gyr, and the collapse timescale is $\sim$ 6.1 Gyr (MS).

There are several factors which enter into the formation of globular clusters (Murray & Lin 1993; Murray et al. 1993). Following Murray et al. (1993), we picture the protogalaxy as comprised of cool dense clouds in pressure equilibrium with a hot intercloud medium from which they have cooled. The first factor which influences the clouds is that they are subject to a Kelvin-Helmholtz (KH) instability which grows as the clouds move through the background gas. This instability leads to the disruption of the clouds on a timescale less than the dynamical collapse time unless their mass exceeds a critical value. Above this critical value, the clouds are gravitationally stabilized and the timescale for the KH instability becomes comparable to the dynamical time. For clouds which survive the KH instability, two possibilities can occur. Clouds with mass in excess of the Jeans mass are subject to a cooling instability (Fall & Rees 1985; Murray & Lin 1989) which leads to rapid star formation and fragmentation or self-regulated star formation. Neither scenario, however, will lead to bound stellar clusters (Murray & Lin 1992). Globular clusters can form, however, from clouds with masses above the critical value (to survive the KH instability) but below the Jeans mass (to avoid spontaneous fragmentation). For our purposes this will correspond to protocluster clouds (PCC's) with masses from 10^4 to $10^6 M_\odot$ (Murray et al. 1993).

For clouds in this mass range three things can occur. The clouds may be compressed, e.g. by cloud-cloud collisions. If the collision is strong enough ($v \gtrsim 10$ km s^{-1}), then the shock will trigger a thermal instability as it passes through a PCC (Murray & Lin 1989; Lin & Murray 1992) and lead to the production of a bound globular cluster. Clouds which experience a collision which is too weak, however, will coagulate and not collapse. Clouds which do not collide are ultimately disrupted by the KH instability. Clearly, the process of globular cluster formation is most efficient for clouds with masses just below the Jeans mass ($\sim 10^6 M_\odot$) which are the easiest to trigger into collapse, but which have the longest lifetime against disruption by interaction with the tenuous background medium.

Following MS, we envision the protogalaxy as initially comprised of protogalactic clouds with mass near the Jeans mass with no subsequent production of clouds in this mass range. For such clouds, the merger rate per cloud is given by eq. [1], while the KH disruption rate per cloud (Murray et al. 1993) is given by

$$\lambda_{\rm KH} \approx \frac{v}{R_{cl} D^{1/2}}, \tag{6}$$

where R_{cl} is the cloud radius (taken here to be an average tidal radius) and D is the density ratio of the clouds relative to the background medium (typically, $D \gg 1$). Assuming pressure equilibrium at the interface between the clouds and the background medium, the density ratio is just related to the ratio of sound speeds in the two media,

$$D^{1/2} \approx \frac{c_1}{c_2} \approx \frac{T_1}{T_2}. \tag{7}$$

The subscripts, 1 and 2, refer to the background and clouds, respectively. We will assume that the cloud temperatures are radiatively cooled to 10^4 K. The background temperature will be just the dynamical temperature of the protogalaxy,

$$T_1 = \frac{m_p v^2}{3k} \tag{8}$$

where m_p is the proton mass. For a typical virial velocity of 200 km s^{-1}, $T_1 \sim 10^6$ K.

Thus, the KH disruption rate can be written as

$$\lambda_{\rm KH} = \frac{v}{R_{cl}} \frac{3kT_2}{m_p v^2} \approx 1.93 \times 10^5 \left(\frac{M_{tot}}{M_\odot}\right)^{-1/6} \left(\frac{m}{M_\odot}\right)^{-1/3} \left(\frac{R_h}{\rm kpc}\right)^{-1/2} \left(1 - e^{-\frac{t-t_0}{t_{vir}}}\right) {\rm Gyr}^{-1}, \tag{9}$$

taking into account the finite timescale for virializationOA. Here R_h denotes the radius of the Galactic halo given by MS. The radius of the halo as a function of time is plotted in Fig. 1.

In order to describe appropriately the evolution of the number and mass of protogalactic clouds (PGC's) represented by $N(t)$ and $m(t)$, the number of protocluster clouds (PCC's) N_{pcc}, the mass of which is $\sim 10^6 M_\odot$, and globular clusters N_{gc}, we need to define the following quantities. First, we define an auxiliary variable $f(t)$ as

$$f(t) \equiv \frac{m_0}{m(t)}. \tag{10}$$

Subsequently we define

$$L_1(t) \equiv \begin{cases} \lambda_m \left\{1 + \epsilon f_{coll} f^{2/3} \frac{N_{pcc}(N_{pcc}-1)}{N(N-1)}\right\} & N_{pcc} > 1 \\ \lambda_m & N_{pcc} \leq 1, \end{cases} \tag{11}$$

$$L_2(t) \equiv \begin{cases} \lambda_m \left(\frac{N}{N-1}\left(\frac{1+f^{1/3}}{2}\right)^2 + \frac{f^{2/3}}{N-1}(N_{pcc}-2)\right\} & N_{pcc} > 2 \\ \lambda_m \frac{N}{N-1}\left(\frac{1+f^{1/3}}{2}\right)^2 & N_{pcc} \leq 2, \end{cases} \tag{12}$$

and

$$L_3(t) \equiv \begin{cases} \lambda_m \left\{1 - \epsilon f_{coll} f^{2/3} \frac{N_{pcc}(N_{pcc}-1)}{N(N-1)}\right\} & N_{pcc} > 1 \\ \lambda_m & N_{pcc} \leq 1. \end{cases} \tag{13}$$

The above three quantities are basically merger rates modified by phase space factors and the production of globular clusters, as we shall see later. Here, f_{coll} is the fraction of a Maxwell-Boltzmann cloud velocity distribution with a relative velocity in excess of the trigger velocity

($\sim 10\ \mathrm{km\,s^{-1}}$). Since the characteristic virial velocities (eq. [2]) considered here are generally large compared to the trigger velocity, this fraction can be taken as near unity. The factor ϵ is the efficiency of globular cluster production.

With these definitions, we have first

$$\frac{dN}{dt} = -(L_1 + \lambda_{\rm KH})N, \tag{14}$$

$$\frac{dN_{pcc}}{dt} = -(L_2 + \lambda^0_{\rm KH})N_{pcc}, \tag{15}$$

where $\lambda^0_{\rm KH}$ is KH disruption rate with $m = 10^6 M_\odot$, and

$$\frac{dN_{gc}}{dt} = \epsilon f_{coll} L_2 N_{pcc}. \tag{16}$$

The interpretations are as follows: L_1 (L_2) describes the decrease in number of PGC's (PCC's) due to mergers and production of globular clusters. Since the PGC system consists of clouds with a spectrum of masses with the average mass of $m(t)$ while the PCC's are clouds of mass $m_0 = 10^6 M_\odot$ by fiat, the merger rates and KH disruption rates for the evolution of the two systems are different. The globular cluster production rate is described by the efficiency (ϵ), the Maxwell-Boltzmann factor (f_{coll}), and the merger rate ($L_2 N_{pcc}$). Since we do not know the efficiency for globular cluster production via this mechanism, we leave it as a free parameter to be determined by other constraints.

With these equations, and the supposition that no new PCC's are formed after their initial appearance, the number of PGC's and PCC's at time t are just

$$N(t) = N(0) \exp\left(-\int_{t_0}^{t} (L_1 + \lambda_{\rm KH}) dt'\right), \tag{17}$$

and

$$N_{pcc}(t) = N(0) \exp\left(-\int_{t_0}^{t} (L_2 + \lambda^0_{\rm KH}) dt'\right). \tag{18}$$

The mass evolution equations are modified from those in MS as

$$\frac{dm_g}{dt} = \left(L_1 - (1-R)\psi - \epsilon f_{coll} L_2 \frac{N_{pcc}}{N}\right) m_g, \tag{19}$$

and

$$\frac{dm_*}{dt} = -\left(L_3 + \epsilon f_{coll} L_2 \frac{N_{pcc}}{N}\right) m_* + (1-R)\psi m_g. \tag{20}$$

The first term in the braket in eq. [19] describes the mass increase due to mergers, the second term mass loss by star formation, and the third term mass loss by production of globular clusters. Eq. [20] can be interpreted in a similar way.

Therefore, eqs. [14], [15], [16], [19], and [20] are the evolution equations that describe the Galactic halo system.

3 Results

3.1 Main results

There are two different points of view as to the mechanism by which globular clusters obtain their metallicities: self-enrichment schemes and previously enriched environments. The fact that the metallicity within most globular clusters is very uniform and that the metallicity of clusters is not much different from that of field stars (see Zinn 1988) argues in favor of environment as fixing the metallicity. Therefore, we adopt the latter view, so we identify the metallicity of the field as that of globular clusters, although self-enrichment may be possible (e.g. Brown et al. 1991). We reproduce the age-metallicity relation of globular clusters and show it in Fig 2. It is compared with the data of Twarog (1980) (see also Colin, Schramm, & Peimbert 1994).

Figs. 3 shows the rate of globular cluster production as a function of time, and Fig. 4 shows the metallicity distribution. For these figures, $\epsilon = 10^{-3}$. In Fig. 4 dN_{gc}/dZ is compared directly to Zinn's data (1985). From Fig. 3, we observe a very distinct epoch of globular cluster formation at the early stage of galaxy formation. Although there exists a second peak at the time of the collapse of the protogalaxy, it is smaller than the first peak by about a factor of 10^7 (we speculate in section 3.2 about processes that might enhance this secondary peak). As for Fig. 4, one can see clearly that the predicted curve is almost identical to the observed metallicity distribution except for the fact that there is no pronounced second peak that corresponds to disk clusters (Zinn 1985, 1988). We will return to the second peak later.

The shape of these curves is unique, i.e. they are insensitive to values of the only free parameter in our model ϵ. Although ϵ enters the equations in a nontrivial way, it does not affect the overall behavior of the system as long as it remains a small parameter. The distribution is largely fixed by the initial burst of globular cluser formation due to the high merger rate when the density of PCC's is highest just after formation. The formation rate then decreases as the protogalactic halo expands (MS). Thus, ϵ changes only the overall amplitude of the globular cluster production, and it can be more or less fixed by the present number of globular clusters. Fig. 5 shows the metallicity distribution curves as ϵ changes from 10^{-1} to 10^{-3}. Table 1 lists values for the final numbers of globular clusters $N_{gc}(T)$, and the coefficients for the quiescent star formation β adjusted to give the present local gas mass fraction of $\mu_g \simeq 0.28$ for different choices of ϵ.

Since the number of globular clusters in our Galaxy is observed to be $\sim$ 100 to 150, then $\epsilon \sim 10^{-3}$ if no significant GC destruction has occurred over the Galactic lifetime.

In addition, our results argue that halo clusters should have a relatively small age spread of less than 1 Gyr and a relatively large metallicity spread. Sandage (1993) determined the ages and the metallicities of 24 Galactic globular clusters. All but one are halo clusters according to Zinn's classification scheme. He reported that the ages of those clusters are 14 ± 1.5 Gyr on the average, and also noted that these clusters have quite small age spread compared to the metallicity spread, which implies that the (halo) globular clusters formed in a short timespan at the very early stage of galaxy formation and the metallicity buildup of our Galaxy was quite fast. This may be regarded tentatively as supporting the conclusion of this model (see also Lee, Demarque, & Zinn 1985).

We point out, however, that measurements of globular age and metallicity have large uncertainties (see Sandage 1993; Chaboyer et al. 1992a, 1992b; VandenBerg, Bolte, & Stetson 1990).

Figs. 6 and 7 shows the numbers of clouds (N, N_{pcc}, N_{gc}) and masses $(m(t), m_g, m_*)$ as functions of time.

We adopted 15 Gyr for the age of our Galaxy as quoted in MS, but since there is a possibility that this might be reduced by as much as a few Gyr (Shi, Schramm, & Dearborn 1994), we examined a few different ages for the Galaxy. As one can find in Fig. 8, the metallcity distribution curve remains virtually unchanged.

We can also consider the case of possible nonbaryonic dark matter (NBDM). If we include NBDM with fixed total mass, we have less baryons than the case of the purely baryonic halo. So we increase the efficiency (ϵ) to 10^{-2} compared with 10^{-3} for purely baryonic halo case. Fig. 9 shows the metallcity distribution curve with 90 % non-baryonic dark matter in the halo. We note that the maximum shifts towards slightly higher metallicity. The purely baryonic halo case, is thus slightly more desirable than NBDM model.

3.2 Absence of the second peak

As was mentioned above, there was no appreciable second peak in the metallicity distribution curve of globular clusters that correspond to disk clusters with higher metallicity. The reason that we didn't get the second peak within the framework of our model is rather straightforward. PCC's, which are progenitors of globular clusters, disappear quite rapidly within a few Gyr of galaxy formation, as one can see in Fig. 6. They turn into globular clusters by starbursts triggered by collisions with other PGC's, merge and coagulate with other clouds, or get disrupted due to KH instability moving through the hot medium. Since the decrease of the number of PCC's is quite rapid, there are not many PCC's when the protogalaxy finally collapses to form the disk. Thus, even though we have a high merger rate again at the time of collapse there is no significant production of globular clusters by this mechanism unless some way is envisaged to prevent total PCC destruction or to form new PCC's during collapse.

However, it is still suggestive that the mean metallicity of the observed second peak, i.e. disk clusters ([Fe/H] $\simeq -0.45$) roughly coincides with the end of the collapse epoch ($t \sim 6$ Gyr) in our model. Therefore, we argue that the disk clusters might form more efficiently than considered here. It seems quite likely, however, that the mechanism that causes the production of disk clusters is associated with the collapse of the protogalaxy. This would require subsequent production of PCC's during or even after the collapse of the protogalaxy.

So this indicates that the two globular cluster populations might have different origins, although they are both triggered by violent motions of gas clouds which induce mergers and collapse.

3.3 Globular clusters in other galaxies: specific frequency

It might be also worthwhile to consider globular clusters in other galaxies. As Ashman & Zepf (1992) already pointed out, elliptical galaxies tend to have many more globular clusters than the same size spirals. If we accept the possibility of mergers of spiral galaxies as one of the leading causes for the formation of elliptical galaxies, this presents a strong case for mergers as sources of globular cluster formation. Ashman & Zepf (1992) also noted, however, that the specific frequency (the number of globular clusters per galaxy luminosity) for a given morphology is almost independent of the mass of the host galaxy. From our calculation we can estimate the approximate dependence of the globular cluster production rate on galactic parameters.

Since the globular cluster production is dominant early on, we need to examine the production rate very early on. From eq. [16] and using the functional approximations used in MS, we have

$$\frac{dN_{gc}}{dt} \propto R_h^{-3/2} M^{11/6}. \tag{21}$$

If we suppose

$$R_h \propto M^{\mu} \quad (\mu > 0),$$

then

$$\frac{dN_{gc}}{dt} \sim M^{\nu}$$

where

$$\nu \simeq -\frac{3}{2}\mu + \frac{11}{6}. \tag{22}$$

The specific frequency of globular clusters for a given host galaxy with mass M, is defined as the number of globular clusters per luminosity. If we suppose that luminosity is proportional to the mass of a galaxy, we have

$$S \equiv \frac{N_{gc}}{L} \propto \frac{N_{gc}}{M} \sim \frac{dN_{gc}/dt}{M} \propto M^{\sigma}. \quad (\sigma = \nu - 1)$$

where

$$\sigma \simeq -\frac{3}{2}\mu + \frac{5}{6}. \tag{23}$$

If radius scales with mass, i.e. $M \propto R^3$, or equivalently $\mu = 1/3$, we have

$$\sigma \simeq \frac{1}{3}. \tag{24}$$

From the above relation, we conclude that the specific frequency S depends weakly, if at all, on the mass of the galaxy. Fig. 10 shows the numerical evaluation of the specific frequency as a function of the galaxy mass for a reasonable range. Actual numerical results confirmed that S indeed depends very weakly on the mass. We find $\sigma \sim 0.12$, which is somewhat smaller than the above analytic estimate. We would like to caution, however, that this is an extremely crude estimate because we assume the same evolution history for galaxies and we do not take into account other mechanisms that affect globular clusters (i.e. subsequent production of disk clusters, disruptions, tidal captures, etc.; Ostriker 1988; Spitzer 1987).

4 Discussion

From the merger model of MS, a model for globular cluster formation arises quite naturally, and we can explain many characteristics of the halo population of globular clusters in our Galaxy in a consistent manner. In particular, we successfully predict the metallicity distribution for globular clusters. This model has the added attraction that it will be testable in the near future and the predictions of the model are robust, i.e. insensitive to choices of parameters. Thus, the merger model seems to be a viable and self-consistent model for galaxy formation.

Previously in MS, we used the instantaneous recycling approximation to simplify the analysis. However, if we abandon the instantaneous recycling approximation, we should employ an appropriate initial mass function (IMF), and the calculations will be improved somewhat (Mathews & Schramm 1994). But the essential features of the model and the prediction in the paper will not change appreciably.

Recently there were observations by ROSAT about the mass fraction of hot gas in rich clusters like Coma cluster (Briel, Henry, & Böhringer 1992; Henriksen & Mamon 1993 for example), and the observed ratio seems to be large considering the scale of the clusters sampled (White et al. 1993) and the constraints on baryonic density from Big Bang Nucleosynthesis (Copi, Schramm, & Turner 1994). The merger model in the context of clusters of galaxies rather than single galaxies might naturally give a plausible explanation for the ROSAT observations as well, and this is investigated in detail in a following paper (Mathews, Charlot, & Schramm 1994).

We would like to thank Sydney van den Bergh for some interesting questions which helped prompt the present paper. We also thank James Truran, Stephen Murray, Douglas Lin, Xiangdong Shi, Geza Gyuk, Bruce Carney, and Pedro Colin for very helpful conversation. The work is performed in part under the auspices of the U.S. Department of Energy by Lawrence Livermore National Laboratory under Contract number W-7405-ENG-48 and Nuclear Theory Grant Number SF-ENG-48. The work is supported at the University of Chicago in part by the DOE, by NASA and by the NSF, and at Fermilab by the DOE and through NASA Grant NAGW 2381. SL acknowledges the support of POSCO Scholarship Foundation in Korea.

ϵ	N_{gc}	β
10^{-3}	3.135×10^{2}	1.985×10^{-4}
10^{-2}	3.134×10^{3}	1.969×10^{-4}
10^{-1}	3.127×10^{4}	1.792×10^{-4}
1	3.020×10^{5}	1.478×10^{-4}

Table 1: Calculated present number of globular clusters N_{gc} and the coefficient of quiescent start formation rate β in units of $\mathrm{Gyr}^{-1}(M_{\odot}/\mathrm{kpc}^{3})^{-1/2}$.

References

Ashman, K. M., & Zepf, S. E. 1992, ApJ, 384, 50.

Briel, U. G., Henry, J. P., & Böhringer, H. 1992, A&A, 259, L31.

Brown, J. H., Burkert, A., & Truran, J. W. 1991, ApJ, 376, 115.

Chaboyer, B., Deliyannis, C. P., Demarque, P., Pinsonneault, M. H., & Sarajedini, A. 1992a, ApJ, 388, 372.

Chaboyer, B., Sarajedini, A., & Demarque, P. 1992b, ApJ, 394, 515.

Colin, P., Schramm, D. N., & Peimbert, M. 1994, ApJ, 426, 459.

Copi, C., Schramm, D. N., & Turner, M. S. 1994, Science, submitted.

Eggen, O. J., Lynden-Bell, D., & Sandage, A. R. 1962, ApJ, 136, 748.

Fall, S. M., & Rees, M. J. 1985, ApJ, 298, 18.

Henriksen, M. J., & Mamon, G. A. 1994, ApJL, in press.

Lin, D. N. C., & Murray, S. D. 1992, ApJ, 394, 523.

Mathews, G. J., Charlot, S., & Schramm, D. N. 1994, in preparation.

Mathews, G. J., & Schramm, D. N. 1993, ApJ, 404, 468 (MS).

Mathews, G. J., & Schramm, D. N. 1994, in preparation.

Murray, S. D., & Lin, D. N. C. 1989, ApJ, 339, 933.

Murray, S. D., & Lin, D. N. C. 1992, ApJ, 400, 265.

Murray, S. D., & Lin, D. N. C. 1993, in Globular Cluster-Galaxy Connection, eds. G. H. Smith, & J. P. Brodie (San Francisco: Astronomical Society of the Pacific), 738.

Murray, S. D., White, S. D. M., Blondin, J. M., & Lin, D. N. C. 1993, ApJ, 407, 588.

Ostriker, J. 1988 in The Harlow-Shapley Symposium on Globular Cluster Systems in Galaxies, eds. J. E. Grindlay, & A. G. D. Philip (Dordrecht: Kluwer), 271.

Peebles, P. J. E., & Dicke, R. H. 1968, ApJ, 154, 891.

Sandage, A. 1993, AJ, 106, 719.

Searle, L., & Zinn, R. 1978, ApJ, 225, 357.

Shi, X., Schramm, D. N., & Dearborn, D. 1994, Physical Review D, 50, in press (August 15).

Spitzer, L. 1987, Dynamical Evolution of Globular Clusters (Princeton: Princeton Univ. Press), 117.

Twarog, B. A. 1980, ApJ, 242, 242.

VandenBerg, D. A., Bolte, M., & Stetson, P. B. 1990, AJ, 100, 445.

White, S. D. M., Navarro, J. F., Evrard, A. E., & Frenk, C. S. 1993, Nature, 366, 429.

Zinn, R. 1985, ApJ, 293, 424.

Zinn, R. 1988 in The Harlow-Shapley Symposium on Globular Cluster System in Galaxies, eds. J. E. Grindlay, & A. G. D. Philip (Dordrecht: Kluwer), 37.

Zinn, R. 1993, in Globular Cluster-Galaxy Connection, eds. G. H. Smith, & J. P. Brodie (San Francisco: Astronomical Society of the Pacific), 38.

Figure Captions

Figure 1.
Radius of the protogalaxy $R_h(t)$ as a function of time (MS).
Figure 2.
Metallicity Z as a function of time. Data points are from Twarog (1980).
Figure 3.
The formation rate of globular clusters dN_{gc}/dt as a function of time with $\epsilon = 10^{-3}$.
Figure 4.
Calculated formation rate of globular clusters dN_{gc}/dZ as a function of metallicity (line) with $\epsilon = 10^{-3}$, compared with data (histogram) from Zinn (1985).
Figure 5.
The formation of globular clusters dN_{gc}/dZ as a function of metallicity for different choices of ϵ. Values of ϵ are $10^{-3}, 10^{-2}, 10^{-1}$, and 1 from left to right. $\epsilon = 10^{-2}$ case is hardly distinguishable from $\epsilon = 10^{-3}$ in the figure.
Figure 6.
Calculated number of protogalactic clouds N (solid curve), protocluster clouds N_{pcc} (dotted), and globular clusters N_{gc} (dashed) as functions of time.
Figure 7.
The average mass m of a PGC (top curve), the average mass m_g in gas of a PGC (middle curve), and the average mass m_* in stellar remnant of a PGC (bottom curve) as functions of time.
Figure 8.
dN_{gc}/dZ as a function of Z for different values of the age of the Galaxy. The solid curve corresponds to 15 Gyr for the age of the Galaxy, the dotted curve 13 Gyr, and the dashed curve 11 Gyr respectively.
Figure 9.
dN_{gc}/dZ as a function of Z, with and without non-baryonic dark matter in the halo. $\epsilon = 10^{-3}$ for the purely baryonic case (solid curve), and $\epsilon = 10^{-2}$ for the non-baryonic case (dotted curve).
Figure 10.
The specific frequency S of globular clusters as a function of the galaxy mass, assuming $\mu = 1/3$ and $\epsilon = 10^{-3}$.

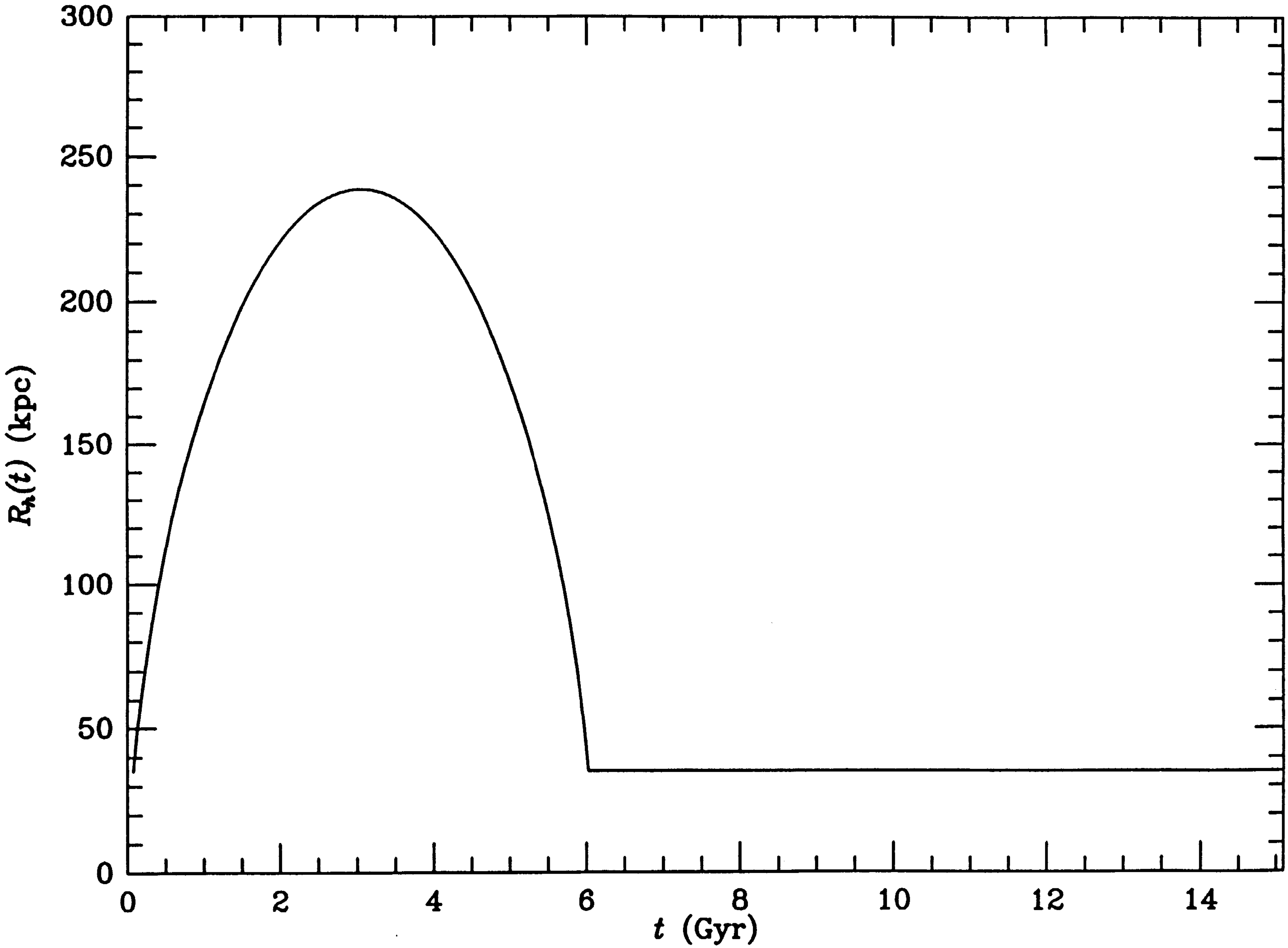

Fig. 1

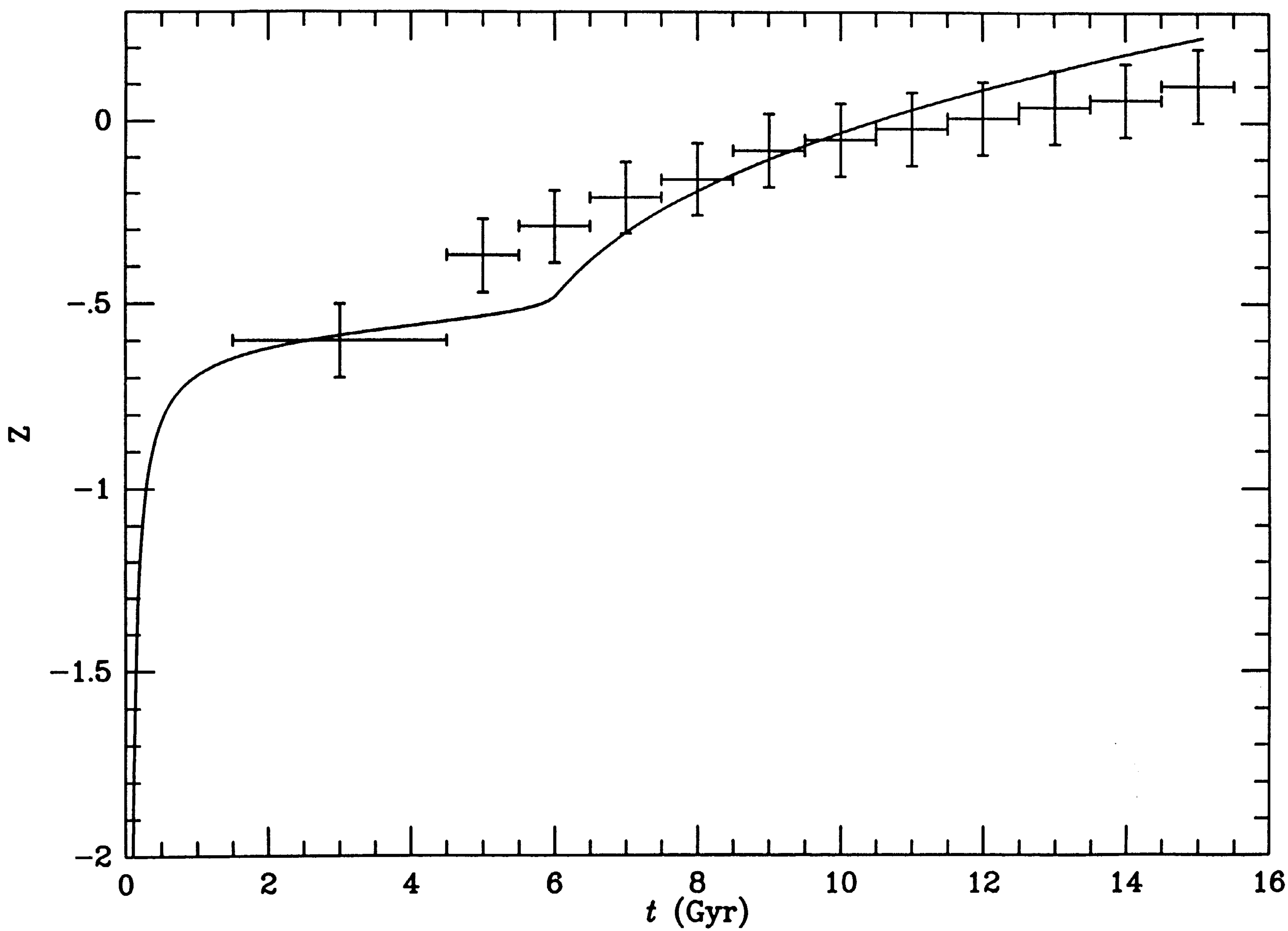

Fig. 2

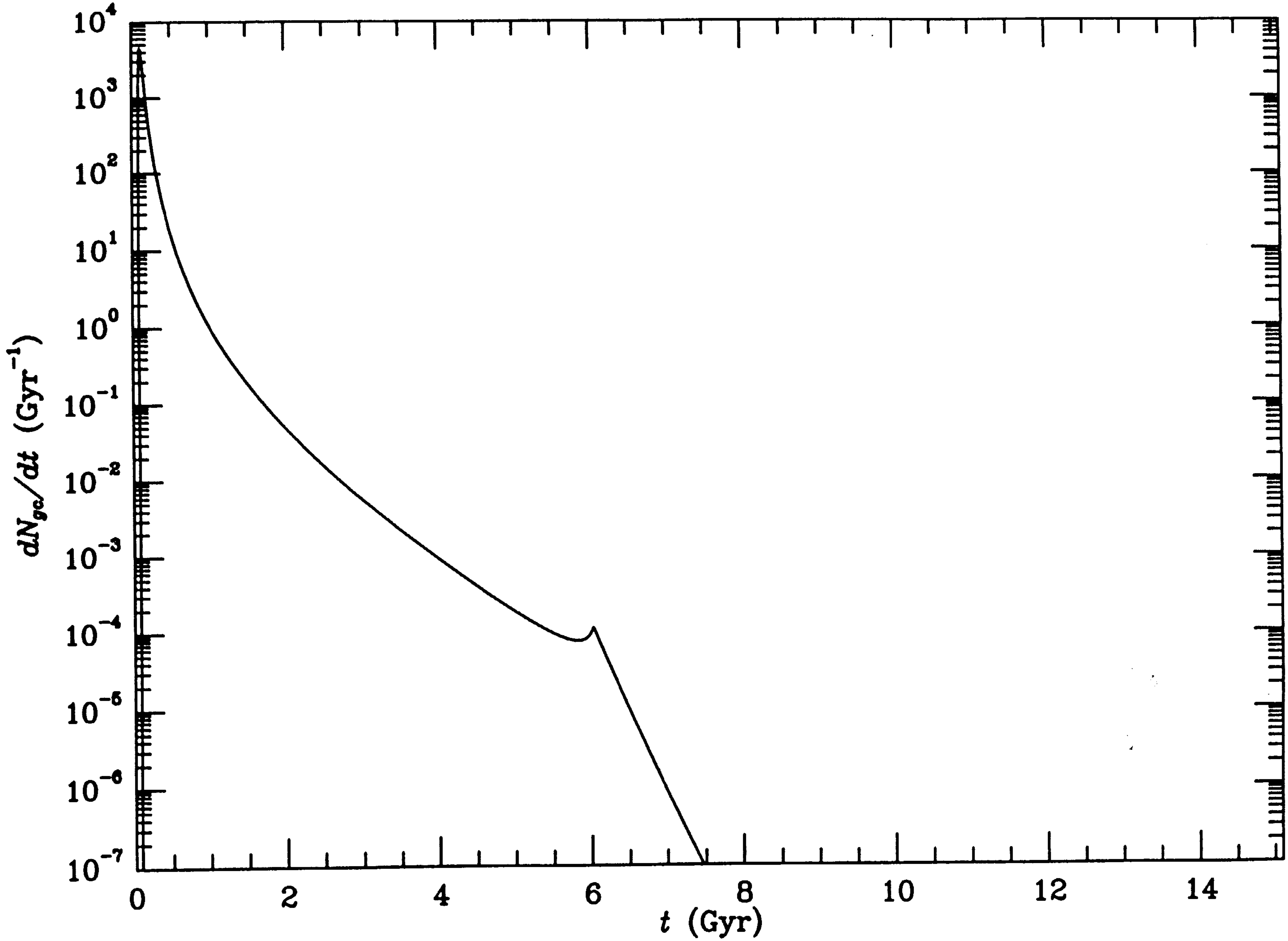
10^4
10^3
10^2
10^1
10^0
10^{-1}
10^{-2}
10^{-3}
10^{-4}
10^{-5}
10^{-6}
10^{-7}
dN_{gc}/dt (Gyr^{-1})
0
2
4
6
8
10
12
14
t (Gyr)

Fig. 3

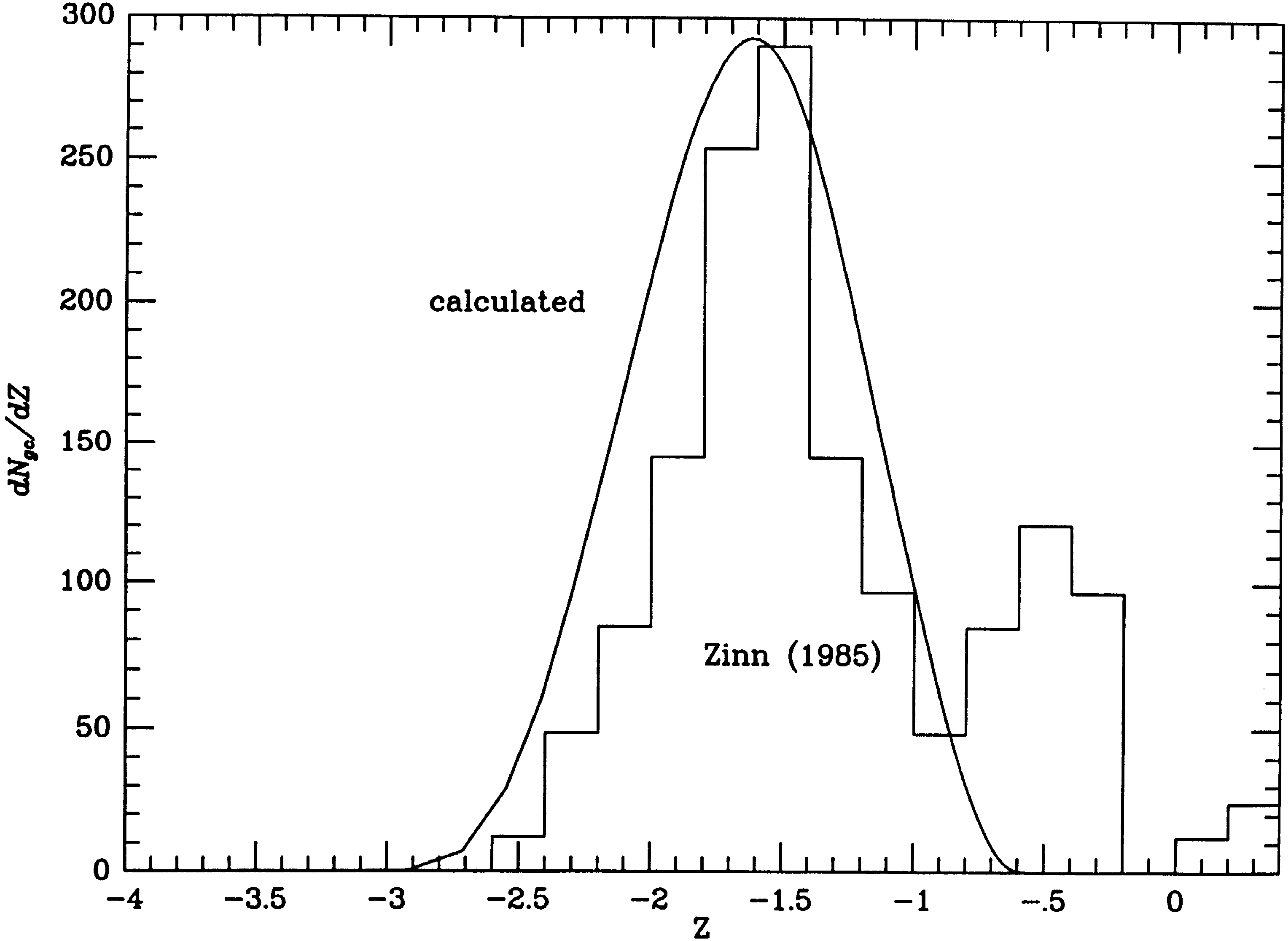
calculated
Zinn (1985)
dN_gc/dZ
Z
300
250
200
150
100
50
0
−4
−3.5
−3
−2.5
−2
−1.5
−1
−.5
0

Fig. 4

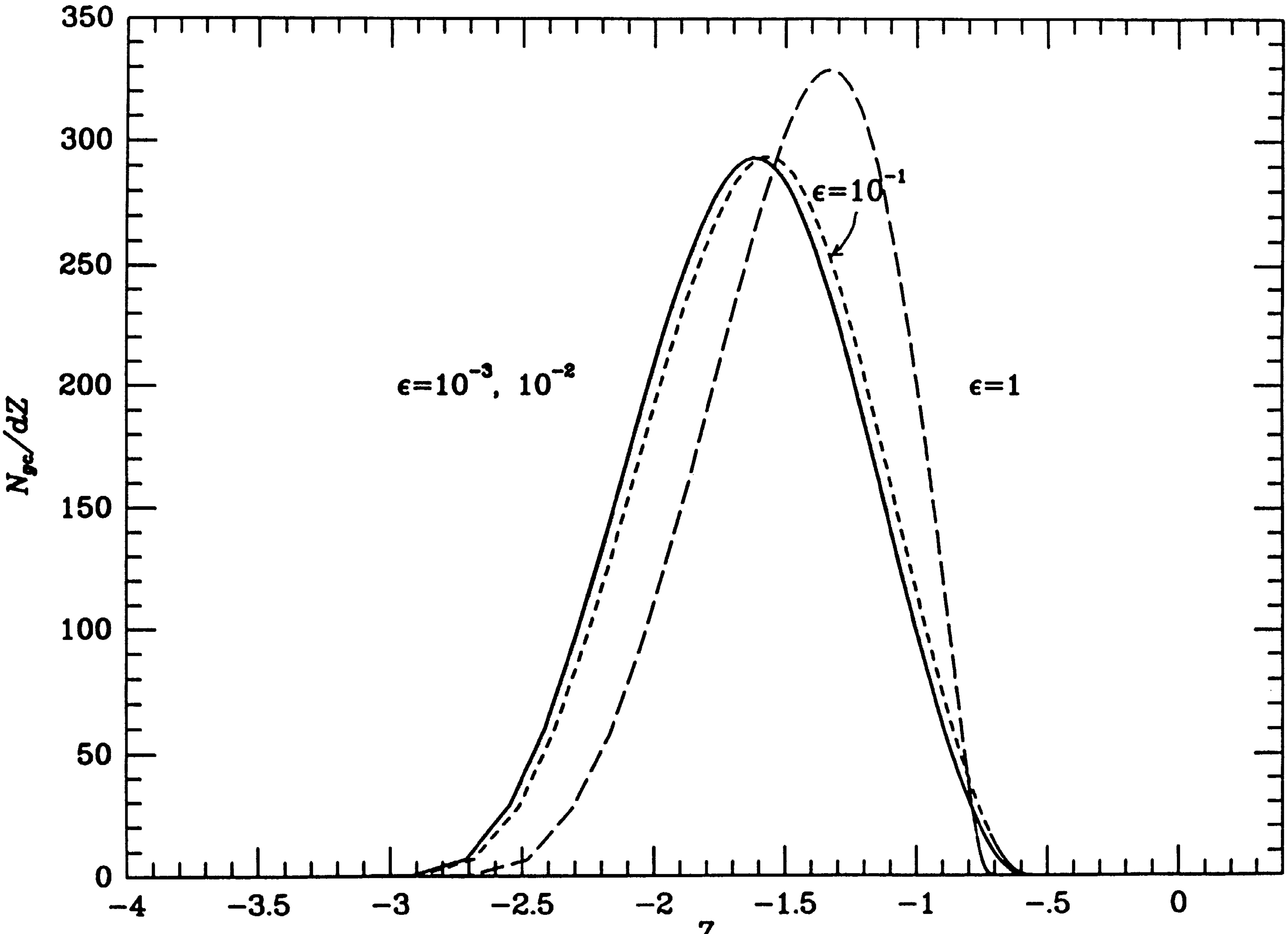

350
300
250
200
150
100
50
0
N_{gc}/dZ
−4
−3.5
−3
−2.5
−2
−1.5
−1
−.5
0
Z
$\epsilon=10^{-3}$, 10^{-2}
$\epsilon=10^{-1}$
$\epsilon=1$

Fig. 5

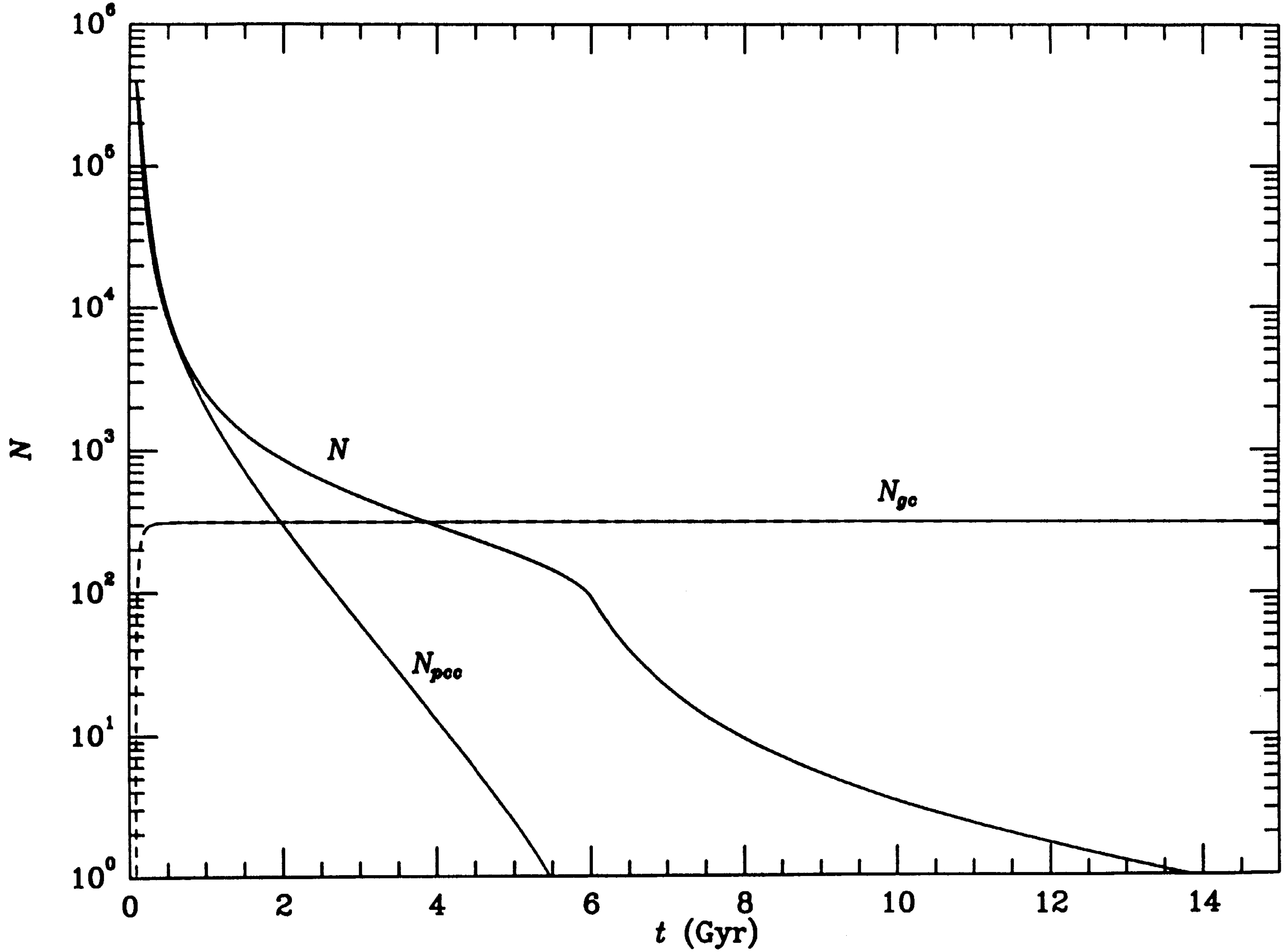

Fig. 6

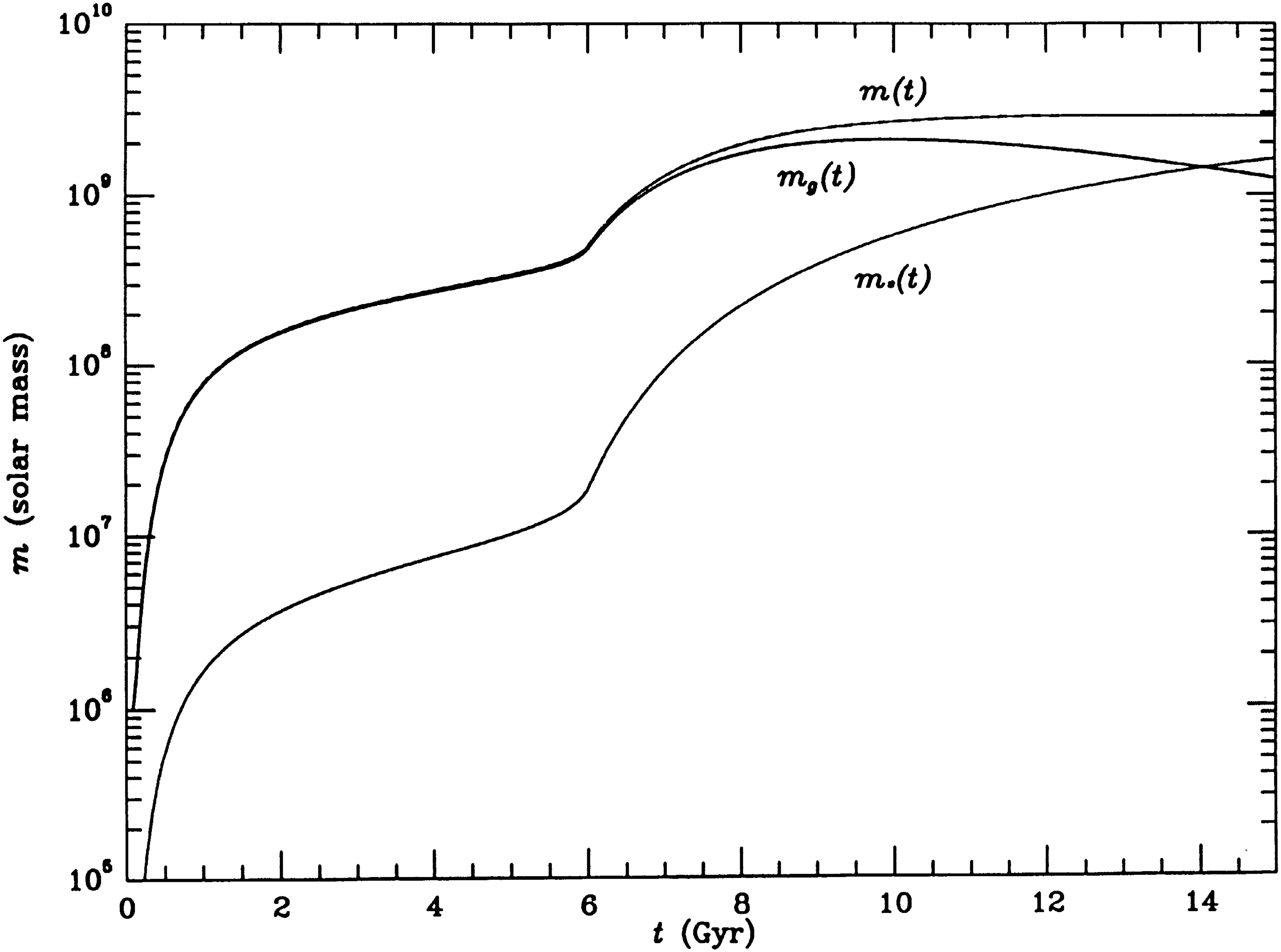
m(t)
m_g(t)
m_*(t)
10^10
10^9
10^8
10^7
10^6
10^5
m (solar mass)
0
2
4
6
8
10
12
14
t (Gyr)

Fig. 7

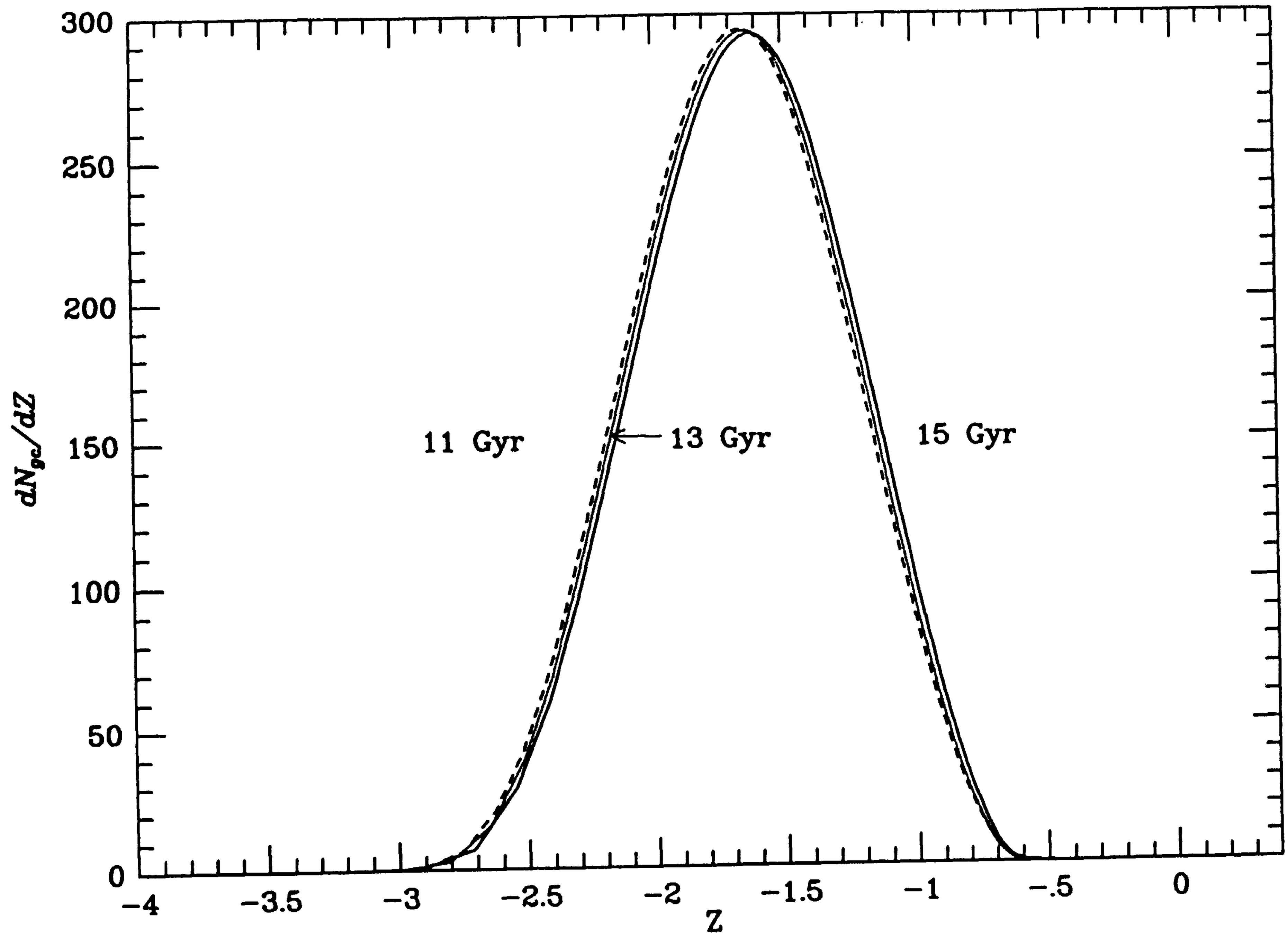

11 Gyr
13 Gyr
15 Gyr
dN_{gc}/dZ
Z
300
250
200
150
100
50
0
-4
-3.5
-3
-2.5
-2
-1.5
-1
-.5
0

Fig. 8

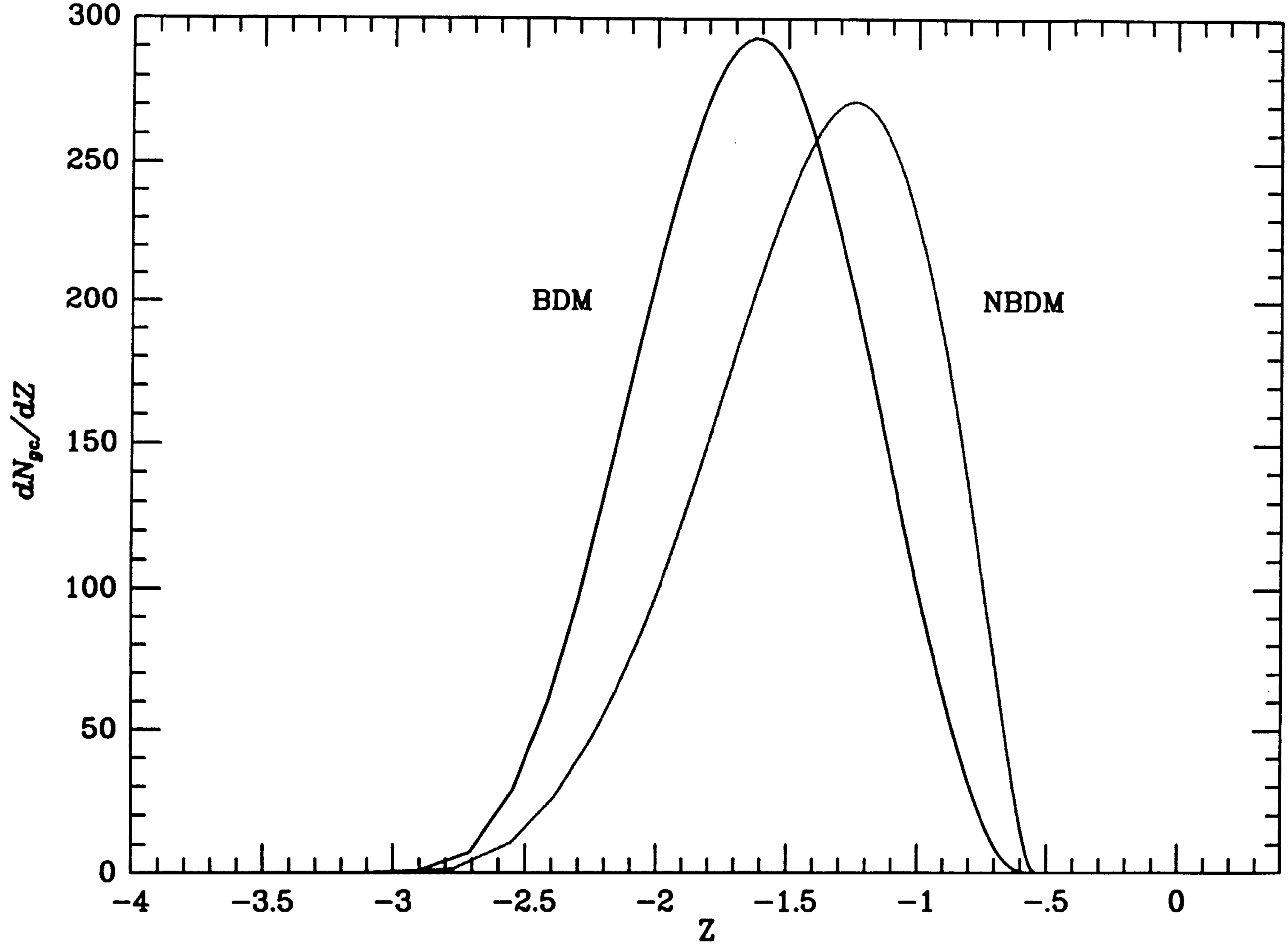

Fig. 9

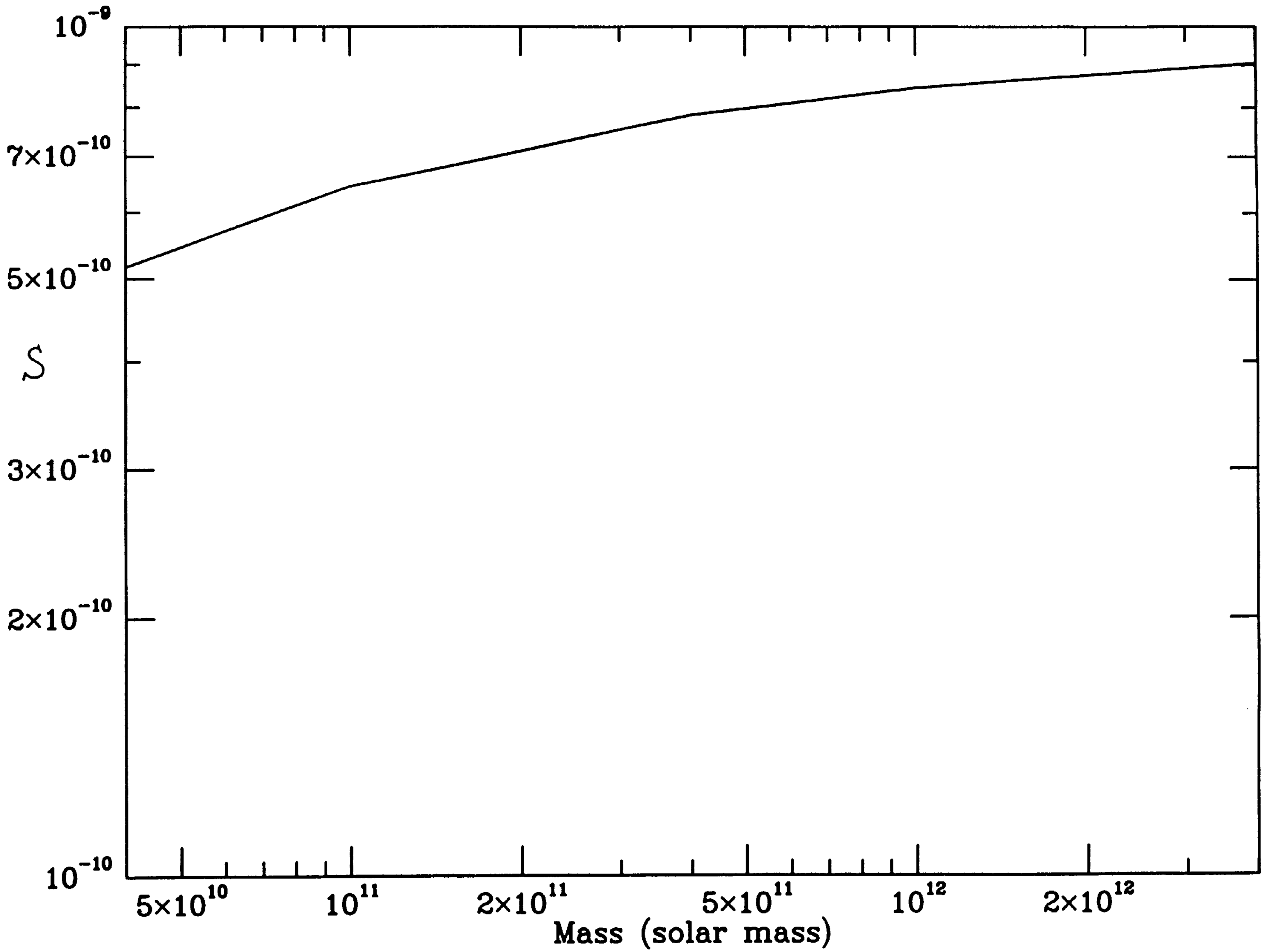

10^{-9}
7×10^{-10}
5×10^{-10}
S
3×10^{-10}
2×10^{-10}
10^{-10}
5×10^{10}
10^{11}
2×10^{11}
5×10^{11}
10^{12}
2×10^{12}
Mass (solar mass)

Fig. 10